Pol. J. Environ. Stud. Vol. XX, No. X (XXXX), 1-13

DOI: *10.15244/pjoes/221721* ONLINE PUBLICATION DATE: 2026-09-18

Original Research

Mapping Forest Disturbances in the Qinling Mountains Using Multi-Source Satellite Data Fusion

Zengnan Li*

College of Geomatics, Xi'an University of Science and Technology, China

Received: 15 November 2025
Accepted: 11 May 2026

Abstract

To overcome limitations in long-term forest disturbance monitoring in mountainous areas arising from persistent cloud contamination and observation sparsity, this study proposed a forest disturbance identification method based on multi-source satellite data fusion, combining Landsat and Sentinel spectral time-series data (2014-2023) in the Qinling Mountains and employing an optimized LandTrendr parameter scheme to derive disturbance year, magnitude, and duration, achieving detailed disturbance detection and mapping and validating spatiotemporal consistency using GFC, FAGE products, and visually interpreted reference samples. The results demonstrate that the proposed multi-source data fusion and optimized LandTrendr approach attained an overall accuracy of 96.51% with a Kappa coefficient of 0.908, exhibiting strong agreement with validation data and superior detection performance compared with the single-sensor LandTrendr model. During the period 2014-2023, the total forest disturbance area in the Qinling Mountains reached about 4.01×10^3 km^2, and disturbances were predominantly distributed in foothill zones characterized by elevations near 800 m and slope gradients of 15°-35°. The proposed forest disturbance detection framework and high-precision disturbance products offer valuable support for long-term forest monitoring and sustainable management in regions with complex topography.

Keywords: Qinling mountains, forest disturbance, LandTrendr, Landsat, sentinel, multi-source satellite data fusion

Introduction

As a fundamental element of terrestrial ecosystems, forests are essential for regulating energy exchange, driving biogeochemical cycles, sequestering carbon, and providing habitats for organisms [1]. In recent decades, forest disturbances have become more frequent around the world. This trend is driven by both accelerating climate change and growing human pressures. Natural causes include fires, pests, and drought. Human activities also play a major role, such as selective harvesting and forest clearing. These combined factors have led to widespread changes in forests at both regional and global levels [2, 3]. Such disturbances markedly alter forest ecosystem composition, structure, and function, impairing stand development, inducing large biomass

*e-mail: lznxust@163.com
0009-0008-0691-7449

losses, and strongly influencing forest carbon balance processes, which ultimately destabilize regional ecosystems and weaken ecosystem services [4-6]. As a result, it is important to develop efficient methods for monitoring forest disturbances. These methods should accurately capture key details such as when and where disturbances occur, their intensity, and how long they last. This information is essential for understanding forest changes at both regional and global levels. It also supports ecological management, helps address climate change [7], and contributes to sustainable development strategies [8].

Since 2010, a variety of forest disturbance monitoring algorithms based on long-term Landsat imagery have been proposed and widely applied [9, 10], including representative methods such as Landsat-based Detection of Trends in Disturbance and Recovery (LandTrendr) [11], Breaks for Additive Season and Trend (BFAST) [12], and Continuous Change Detection and Classification (CCDC) [13]. Notably, LandTrendr is capable of detecting slow, long-term forest trends as well as sudden disturbance events, and its computational efficiency, robustness, and accuracy make it particularly well suited for long time-series forest disturbance analyses [11, 14, 15]. Earlier research employing LandTrendr for European forest disturbance mapping has shown that the algorithm performs well across a wide range of terrain slopes. Because conventional LandTrendr implementations depend exclusively on Landsat data, insufficient cloud-free observations can lead to gaps in time series, resulting in missed disturbance detections and inadequate support for fine-scale forest management [16-18]. Despite its later launch, Sentinel-2 offers finer spatial resolution and more frequent effective observations [19, 20]. Integrating Sentinel-2 data into annual composites not only overcomes the shortcomings of single-sensor data acquisition but also at least doubles the availability of high-quality observations [21]. Improved composite image quality enhances the use of temporal context to characterize dynamic forest changes, minimizes missed detections due to data gaps [22], and supports accurate timing and near-real-time monitoring of disturbances, leading to marked improvements in spatiotemporal detection accuracy [23, 24].

Existing research on satellite-based forest disturbance detection has paid limited attention to systematically evaluating how multi-source data fusion can enhance the performance of change detection algorithms when time series are temporally discontinuous [25].

This study aims to assess the effectiveness of forest disturbance monitoring in complex mountainous terrain by fusing multi-source satellite imagery and examining spectral specificity and temporal dynamics [26, 27]. The LandTrendr method does not work as well in complex terrain. It is less effective at detecting subtle disturbances compared to strong ones. This is due to several factors. These include the duration and intensity of the disturbance, the length of the time series, and the algorithm settings [28]. Therefore, adjusting these parameters is necessary to improve the method's sensitivity to weak disturbances [11].

This study focuses on the Qinling Mountains. It aims to improve forest disturbance monitoring in areas with frequent cloud cover. To achieve this, we integrated multi-source satellite time-series data. We systematically analyzed the spectral signals of forest disturbances. Algorithm parameters were also optimized to improve detection sensitivity in complex terrain. These steps helped enhance the LandTrendr method for identifying both the timing and spectral characteristics of disturbances. As a result, we produced high-accuracy disturbance maps. These maps support more precise forest management and the sustainable use of mountain forest resources.

Materials and Methods

Data Sources

Study Area

The Qinling Mountains, situated in central China and southern Shaanxi Province (32°07′-34°44′N, 105°42′-111°01′E), span approximately 71,200 km^2 and exhibit an elevation range of 162-,711 m (Fig. 1). The study area is characterized by a subtropical monsoon climate, with annual mean temperatures of 12-25ºC and precipitation totals ranging from 923 to 2,459 mm. The region includes six prefecture-level cities and is distinguished by high ecosystem diversity and biodiversity, functioning as a key geographic and climatic boundary between northern and southern China [29]. In addition, the Qinling Mountains have a forest coverage of about 70%, dominated by coniferous forest, deciduous broadleaf forest, and shrub vegetation.

In recent decades, both human activities and climate change have led to major changes in forest cover in the Qinling Mountains. These human activities include logging, fires, pest outbreaks, land clearing, and urbanization. As a result, this area has become one of the most frequently disturbed forest regions in Shaanxi Province. By modifying forest ecological structure, growth status, and species composition, forest disturbances markedly reduce ecosystem service capacity and have significant consequences for the local environment.

Remote Sensing Imagery

In this study, multi-source Landsat and Sentinel spectral datasets (2014-2023) obtained from the Google Earth Engine (GEE) cloud platform were employed as the main data sources for forest disturbance monitoring in the Qinling Mountains. Landsat surface reflectance (SR) data from Landsat 5 TM, Landsat 7 ETM+, and Landsat 8 OLI at 30 m spatial resolution were used,

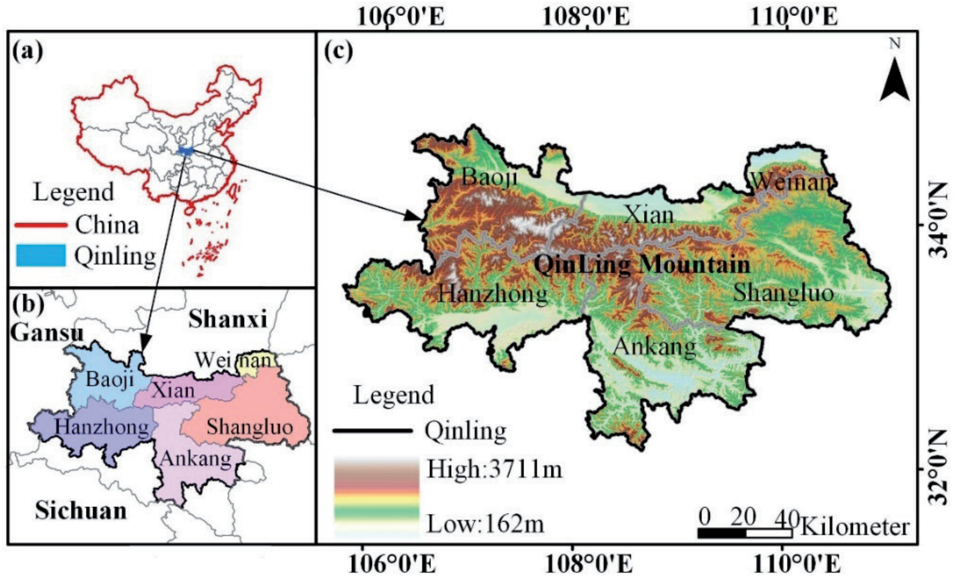

Fig. 1 The study area.

together with Sentinel-2 Level-2A surface reflectance data at 10 m resolution. Deciduous broadleaf forests dominate the Qinling Mountains, where vegetation indices decrease markedly during the leaf-off season in December.

To prevent natural phenological variations from being misidentified as disturbances, the leafy season was defined as March–November, and only cloud-free images acquired during this period were used. Before further analysis, all imagery underwent geometric, radiometric, and atmospheric correction. For consistency between sensors, Sentinel-2 imagery was resampled to 30 m and quality masking was used to exclude clouds, cloud shadows, and snow. Following preprocessing, all valid annual Landsat and Sentinel-2 observations were used to compute spectral indices and were integrated using an optimal pixel compositing approach, effectively reducing cloud effects and inter-sensor spectral differences and producing spatially continuous, gap-free annual multispectral index time-series stacks.

Reference Data

Furthermore, forest disturbance ground samples were randomly identified by visually examining historical and recent high-resolution Google Earth imagery. Candidate forest disturbance samples were first filtered through spectral analysis and multi-temporal visual interpretation, and then further verified and refined using published literature and historical documentation to ensure the authenticity of disturbance events. Overall, 20 wildfire events, 18 harvesting events, and 12 road expansion events were identified, yielding 518 disturbed and 1,433 undisturbed reference sample points when combined with the Global Forest Change dataset and historical records. Each disturbance event encompassed more than 30 pixels (30 m resolution) and was dated between 2014 and 2023.

Forest Disturbance Products

Forest disturbance datasets were sourced from the Global Forest Change (GFC) product and the Chinese Forest Age Dataset (FAGE). Developed from Landsat imagery, the Global Forest Change dataset supplies global forest cover, loss, and gain information for 2001–2023 at 30 m resolution and is extensively used to validate forest disturbance monitoring studies worldwide [9]. The Chinese Forest Age Dataset, produced by machine learning–based integration of multi-source remote sensing data and field observations, covers all forest regions of mainland China at 30 m resolution and enables indirect evaluation of forest disturbance through forest age dynamics.

Research Methods

Overview of Workflow

As shown in Fig. 2, the methodological framework consists of: (1) multi-source satellite data integration and forest baseline mapping, which involves preprocessing, spectral index computation, and fusion of Landsat 5/7/8 and Sentinel-2 multispectral images (2014-2023), generating annual forest baseline maps using a random forest classifier based on fused multi-source data, and masking non-forest pixels in the spectral index time-series stacks using the annual forest masks; (2) forest disturbance detection and mapping, where LandTrendr control parameters are optimized to improve sensitivity to disturbances in mountainous terrain, and forest disturbances are identified using forest-masked, multi-

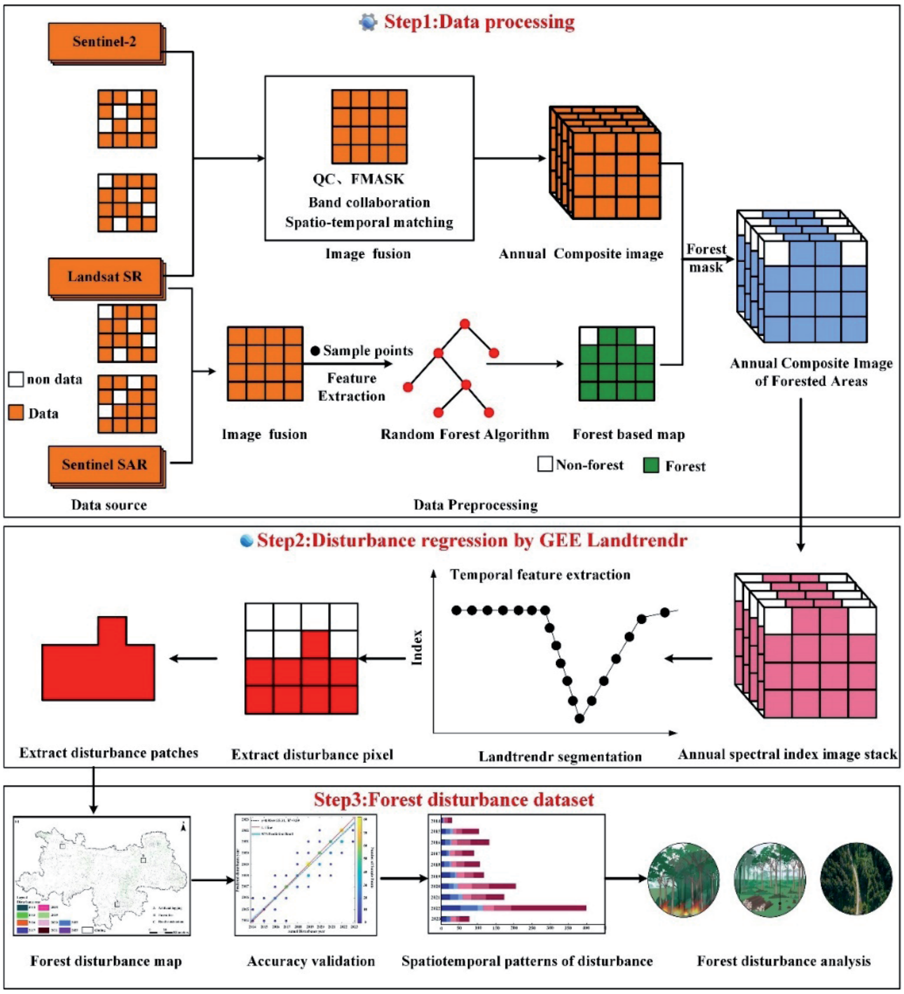

Fig. 2. Overview of workflow.

source fused datasets with LandTrendr, together with accuracy evaluation; (3) spatiotemporal characterization of disturbances, extracting spatiotemporal information on forest pest-related disturbances during 2014-2023 and analyzing their patterns and intensity classes in the Qinling Mountains through trend analysis and a fishnet-based spatial model.

Forest Base Map Generation

This study focuses on historical forest disturbance detection. Therefore, constructing a high-accuracy forest extent map is a prerequisite for conducting LandTrendr analysis. A detailed mountain forest base map not only helps reveal forest structure and dynamic changes, but also plays a crucial role in improving disturbance detection accuracy. However, mountainous regions are characterized by complex land cover types and strong regional variability in remote sensing signals. Existing land cover products often have long temporal coverage but low update frequency. These products cannot fully meet the requirements of fine-scale time-series analysis.

To reduce spectral noise and misclassification caused by non-forest pixels in long-term series, and to account for regional differences and multi-source data integration, we developed an annual forest base map covering the period from 2014 to 2023. The method integrates Landsat optical time-series data, Sentinel-1 SAR data, forest structural features, and machine learning algorithms. This approach ensures consistency with the disturbance monitoring period and enables the construction of a high-precision forest mask.

The detailed procedure is as follows. Cloud-free Landsat 5/7/8 images during the growing season were acquired annually from Google Earth Engine (GEE). Starting from 2016, Sentinel-1 SAR data were incorporated to enhance classification performance under cloudy conditions. All images underwent radiometric calibration, atmospheric correction, orthorectification, and cloud and noise removal.

Spectral indices were then calculated, including the Normalized Difference Vegetation Index (NDVI), Enhanced Vegetation Index (EVI), Normalized Difference Water Index (NDWI), and Normalized Difference Built-up Index (NDBI). Radar backscatter features were extracted from VV and VH polarizations. Texture features were derived using gray-level statistical measures. Feature selection was conducted based on mean squared error. Finally, 25 key variables were retained for model construction.

Training samples were collected through visual interpretation of high-resolution imagery and existing forest products. These samples covered the main land cover types. A Random Forest classifier was applied to generate ten annual forest maps at 30 m spatial resolution.

The annual forest base maps are fully consistent with the LandTrendr processing framework. Disturbance detection was therefore restricted to confirmed forest areas. This approach effectively reduced spectral noise and improved the stability and reliability of disturbance time-series identification.

Detecting Forest Disturbances Using the Landtrendr Algorithm

LandTrendr analyzes each pixel's time series by setting parameters such as spike threshold, vertex count overshoot, trajectory fitting, p-value threshold, and the best model proportion. This approach captures critical phases such as disturbance onset, prolonged degradation, and recovery in the time series, enabling the detection of sudden, progressive, or long-term forest disturbance features. The algorithm can select different spectral indices for detection, and among them, NBR is highly sensitive to changes in chlorophyll content, canopy water content, and carbon ash, effectively reflecting both degradation and recovery processes. Therefore, NBR was selected as the primary input indicator for this study.

$$\mathrm{NBR}=\frac{\mathrm{NIR\text{-}SWIR2}}{\mathrm{NIR+SWIR2}} \tag{1}$$

where NIR and SWIR2 refer to the near-infrared (850-880 nm) and shortwave infrared (1570-1650 nm) band reflectance from Landsat and Sentinel-2 imagery, respectively.

The conventional LandTrendr algorithm relies on Landsat satellite data, but in the Qinling region, frequent cloud cover, rain, and terrain obstruction prevent a single satellite from providing high-quality cloud-free observations, resulting in fewer fitting segments and missed disturbance signals. This study combines Landsat and Sentinel-2 data to improve the continuity and stability of the time series. It uses annual forest baseline maps to mask out non-forest areas. This process creates continuous, stable, and cloud-free annual spectral data for forested regions. The result is high-quality data that supports accurate disturbance identification. Given the high frequency of forest disturbances, fast recovery rates, and multiple overlapping disturbances in the Qinling region, the default LandTrendr parameters remain inadequate for sensitivity in detection when applied to high-quality time series data. The study utilized the control variable method to test multiple disturbance plots and specifically optimized key parameters. By increasing max Segments and vertex count overshoot, the model is able to parse more fitting segments and differentiate between consecutive or overlapping disturbance events. Given that some pest-related disturbances in Qinling may degrade and recover within a single year, the recovery Threshold was set to 1, and the Prevent One-Year Recovery parameter was set to false. This configuration enhances sensitivity to weak disturbances and prevents the default settings from ignoring fast recovery events within a year. The parameters of the improved LandTrendr algorithm are provided in Table 1 [30].

Accuracy Assessment

The algorithm's accuracy in this study is assessed from three perspectives: data sources, overall accuracy, and forest disturbance products. To examine how the choice of data sources affects disturbance monitoring, single-source Landsat and multi-source fused Landsat–Sentinel-2 datasets were used as inputs to the parameter-optimized LandTrendr algorithm. Detection of disturbance years and areas under cloud cover and terrain shadow conditions was compared to assess the performance of multi-source data fusion. In addition, overall accuracy was assessed based on reference sample points. We calculated several accuracy metrics for forest disturbance detection. These included producer accuracy, user accuracy, and overall accuracy. The calculations were based on reference sample points from both stable and changing forests. Confusion matrices were used to compute these metrics, with precision further quantified by commission error, omission error, and F1 score. The formulas are expressed as:

$$\mathrm{commission}=\frac{\mathrm{FP}}{\mathrm{FP+TP}}\times 100\% \tag{2}$$

$$\mathrm{omission}=\frac{\mathrm{FN}}{\mathrm{FN+TP}}\times 100\% \tag{3}$$

Table 1. Parameter settings of the LandTrendr algorithm.

Parameter	Parameter Value	Parameter Optimization
Max Segments	8	6
Spike Threshold	0.90	0.5
Vertex Count Overshoot	0	5
Prevent One-Year Recovery	True	false
Recovery Threshold	0.50	0.5
Pval Threshold	0.05	0.05
Best Model Proportion	0.75	0.05
Min Observations Needed	5	4
Magnitude	≥0.17	≥0.17

$$\mathrm{F1\_score} = \frac{2\times \mathrm{TP}}{2\times \mathrm{TP}+\mathrm{FP}+\mathrm{FN}} \times 200\% \quad (4)$$

where commission error represents false positives (FP), or undisturbed areas incorrectly classified as disturbed, omission error corresponds to false negatives (FN), or disturbed areas that were missed, and true positives (TP) denote areas correctly identified as disturbed. The F1-score is calculated based on TP, FP, and FN. It provides a balanced measure of classification accuracy, with higher values indicating better agreement with reference data.

Furthermore, to assess the accuracy of the forest disturbance products produced in this study, existing 30 m global forest change and China forest age datasets were used for comparison. Although these datasets show good local-scale accuracy, their performance for monitoring forest disturbances in the Qinling Mountains has not been previously validated.

For forest disturbance product validation, linear regression and correlation analyses were performed comparing the disturbance years from the forest disturbance products, the LandTrendr algorithm outputs, and actual disturbance years from visual interpretation, to assess the effectiveness of the multi-source satellite fusion-based products in mountainous areas.

Spatiotemporal Analysis of Forest Disturbances

Using administrative boundaries, elevation, and other fundamental geographic data of the Qinling Mountains, the GEE platform was employed to assess the spatiotemporal patterns of forest disturbances from 2014 to 2023 and their distribution along various elevation and slope gradients. Slopes were classified into six levels: flat (0°-5°), gentle (5°-15°), moderate (15°-25°), steep (25°-35°), very steep (35°-45°), and extreme (>45°). Elevation was categorized into five ranges with thresholds at 800 m, 1450 m, 2100 m, and 2750 m. Furthermore, a fishnet grid was applied to partition the study area for analysis of disturbance level distribution.

Results and Discussion

Spatiotemporal Changes of Forests in the Qinling Mountains

Non-forest pixels may compromise the accuracy of LandTrendr-based disturbance detection; masking out non-forest areas like croplands and grasslands prevents high false positive rates. Landsat optical images and Sentinel-1 SAR data were fused in this study, incorporating spectral, radar, and texture characteristics. Subsequently, annual training samples were classified using a random forest classifier, producing a 30 m resolution annual land cover dataset for the Qinling Mountains from 2014 to 2023. The classification attained an overall accuracy exceeding 90% and a Kappa coefficient greater than 0.9, and by masking non-forest pixels, annual forest baseline maps were produced for the study period.

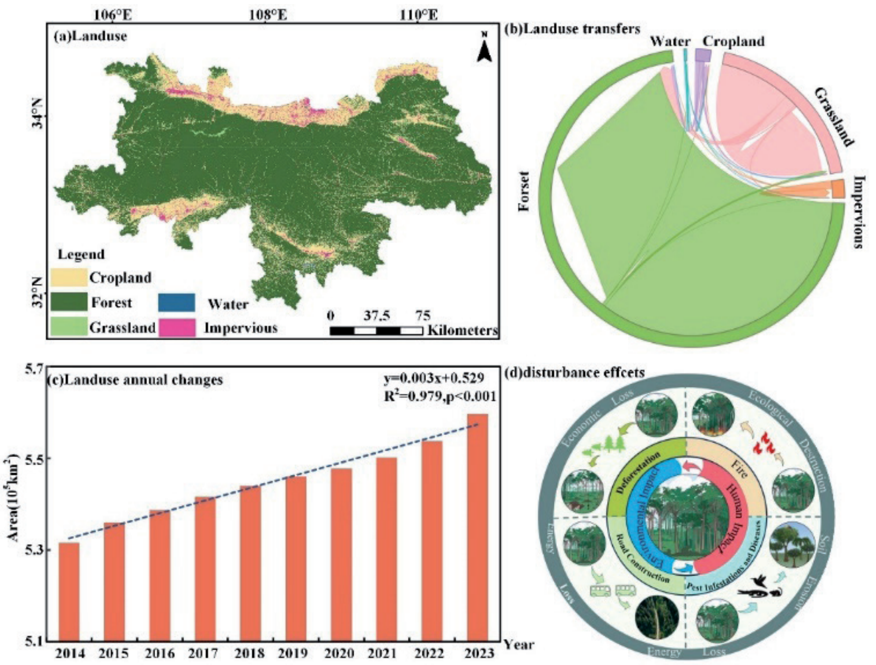

Fig. 3. Land cover changes and forest base maps in the Qinling Mountains from 2014 to 2023. a) Land use in the Qinling Mountains in 2023; b) Land cover transitions from 2014 to 2023; c) Annual changes in forest area; d) Driving factors of forest disturbances in the Qinling Mountains.

Fig. 3 indicates that forest coverage in the Qinling Mountains has been steadily increasing. Under the implementation of ecological restoration policies, including “returning farmland to forest”, forest coverage reached 82.7% by 2023. The comparison of land cover changes from 2014 to 2023 indicates that the primary forest transformations in Qinling over the last decade were forest-to-cropland and forest-to-construction land conversions, totaling 495.16 km^2 and 2.65 km^2, respectively, representing approximately 0.9% of the 2023 forest area. Based on historical surveys of forest disturbances in the Qinling Mountains, natural factors including pest outbreaks and wildfires, alongside anthropogenic activities such as logging and urban development, are the primary drivers of forest disturbances, causing ecological degradation, soil erosion, and substantial ecological and economic damage.

Consequently, establishing rapid monitoring methods for forest disturbances is crucial for forest research and serves as an important reference for forestry management policy formulation.

Comparative Analysis of the Two Algorithm Outcomes

Accuracy assessment was conducted using 1951 reference points derived from visual interpretation to evaluate the results of the multi-source satellite data fusion with LandTrendr parameter optimization, and a scatter plot was created. The results in Fig. 4 indicate that the disturbance years detected by the improved method closely match the reference years obtained through visual interpretation. The majority of observation points lie close to the 1:1 line, with a linear regression slope of 0.93 and an R^2 of 0.89, demonstrating that multi-source satellite fusion time series effectively enhanced the temporal accuracy of disturbance detection (Fig. 5). A slight overestimation occurs in some events, attributed to spectral disturbances in the early stages of vegetation recovery, causing interpretive bias.

These results suggest that the method is highly reliable for detecting stable forest regions and exhibits greater sensitivity to long-lasting, high-intensity

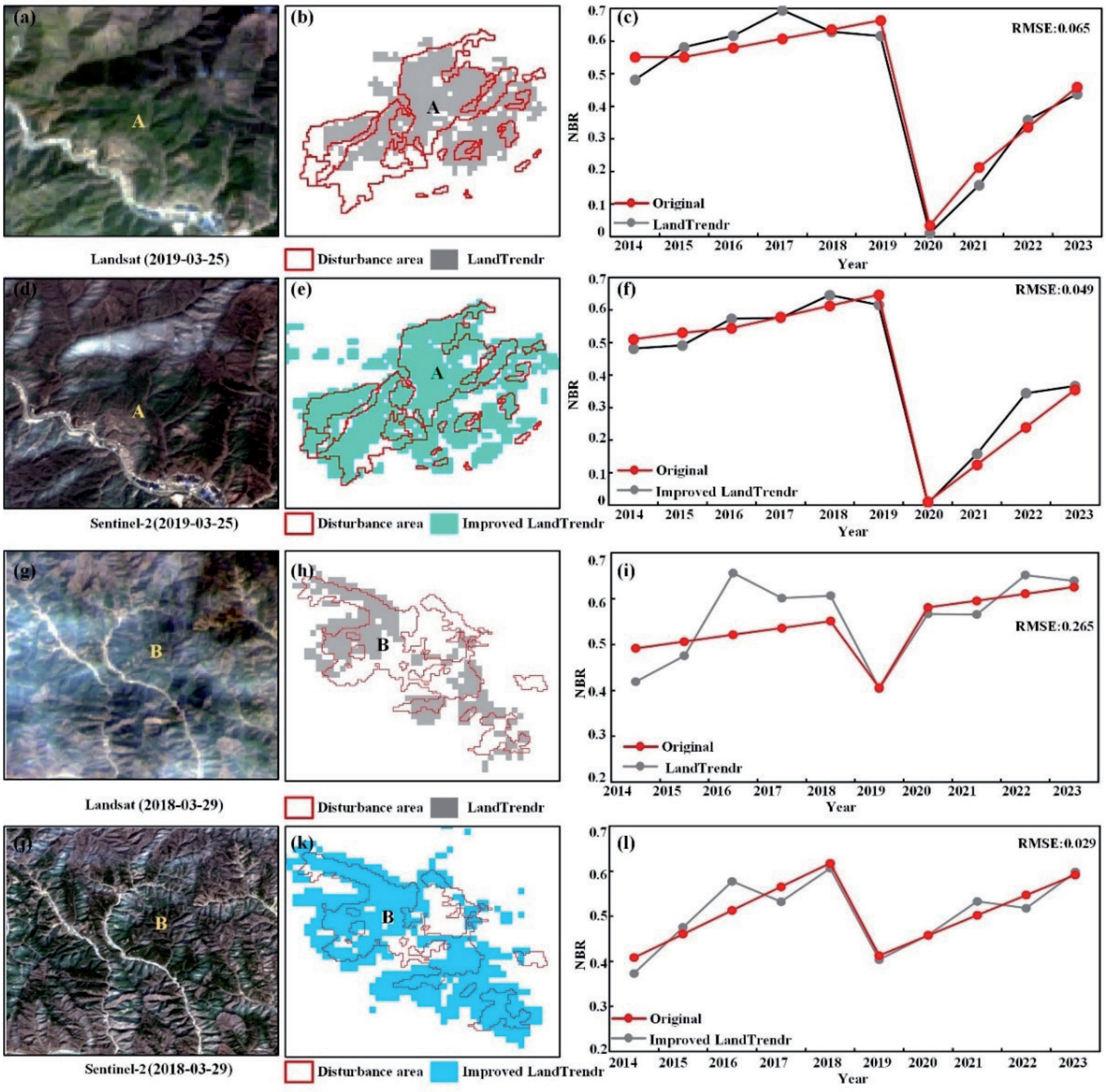

Fig. 4. Comparative analysis of the two algorithm outcomes.

Table 2. Confusion matrix of LandTrendr-based forest disturbance classification derived from validation samples.

Detection	Reference sample		User's accuracy (%)
	Undisturbed	Disturbed	
Undisturbed	1408	45	91.3%
Disturbed	25	473	94.9%
(Production's accuracy (%)	98.3%	96.9%	_
(%)	96.5%		
Kappa	0.908		

disturbances, but the use of annual fused data imposes certain limitations on identifying sudden and short-lived events like pest outbreaks.

Evaluation of Overall Accuracy

To further assess the benefits of integrating multi-source satellite data fusion with LandTrendr parameter optimization for identifying spatiotemporal disturbance information, the outputs of the improved method were cross-validated with GFC and FAGE forest disturbance products derived from single-source Landsat data. For temporal accuracy comparison, disturbance years were extracted for reference sample points across different disturbance products and the improved method, followed by point-by-point comparison. The improved method attained the highest temporal accuracy (R^2 = 0.76), surpassing GFC (R^2 = 0.72) and greatly outperforming FAGE (R^2 = 0.26).

Subsequently, classification accuracy was further assessed by constructing a confusion matrix based on the same set of reference samples. As shown in Table 2, the user's accuracy reached 91.3% for undisturbed areas and 94.9% for disturbed areas, with producer's accuracies of 98.3% and 96.9%, respectively; the overall F1 score was 94.6% and the commission error was as low as 1.74%, demonstrating strong classification robustness and high sensitivity to moderate and severe disturbance events. Overall, the results suggest that the proposed approach reliably identifies stable forest areas and exhibits higher sensitivity to long-lasting and high-intensity disturbances; however, the use of annual fused time-series data imposes certain limitations in capturing abrupt and short-lived disturbances, such as insect infestations.

Comparison with Existing Forest Disturbance Products

The results (Fig. 6) reveal that single-source products have biases in regions with missing or interrupted observations, demonstrating that multi-source fusion

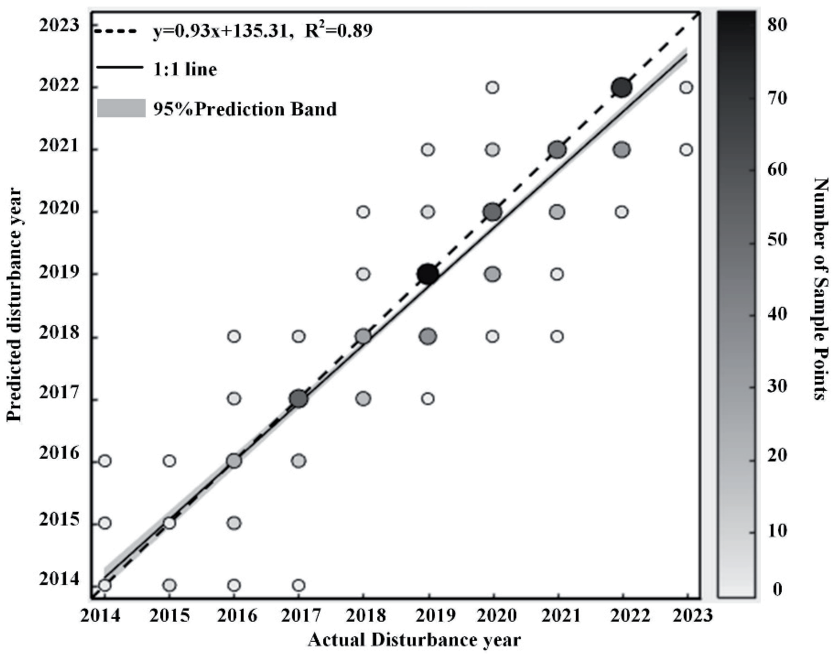

Fig. 5. Accuracy assessment of forest disturbance detection.

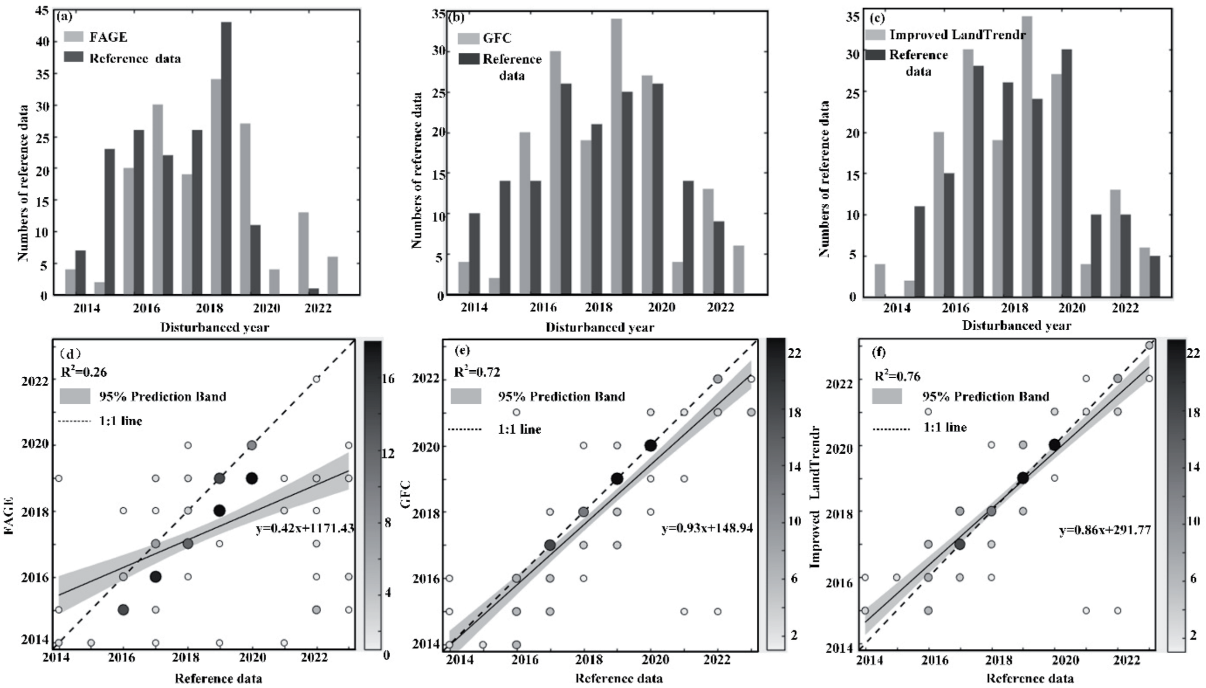

Fig. 6. Comparison of disturbance year detection among different products.

markedly enhances the continuity of time series and the precision of disturbance event identification. Compared with single-sensor approaches, it delivers more robust and noise-resilient temporal trajectories.

Three representative disturbance cases were selected to assess the spatial detection capability, and the improved method's results were compared with those from GFC and FAGE products. As shown in Fig. 7, for large and persistent disturbance events, the improved model provides the most accurate spatial delineation, GFC shows moderate performance, and FAGE tends to underestimate small-scale or short-duration

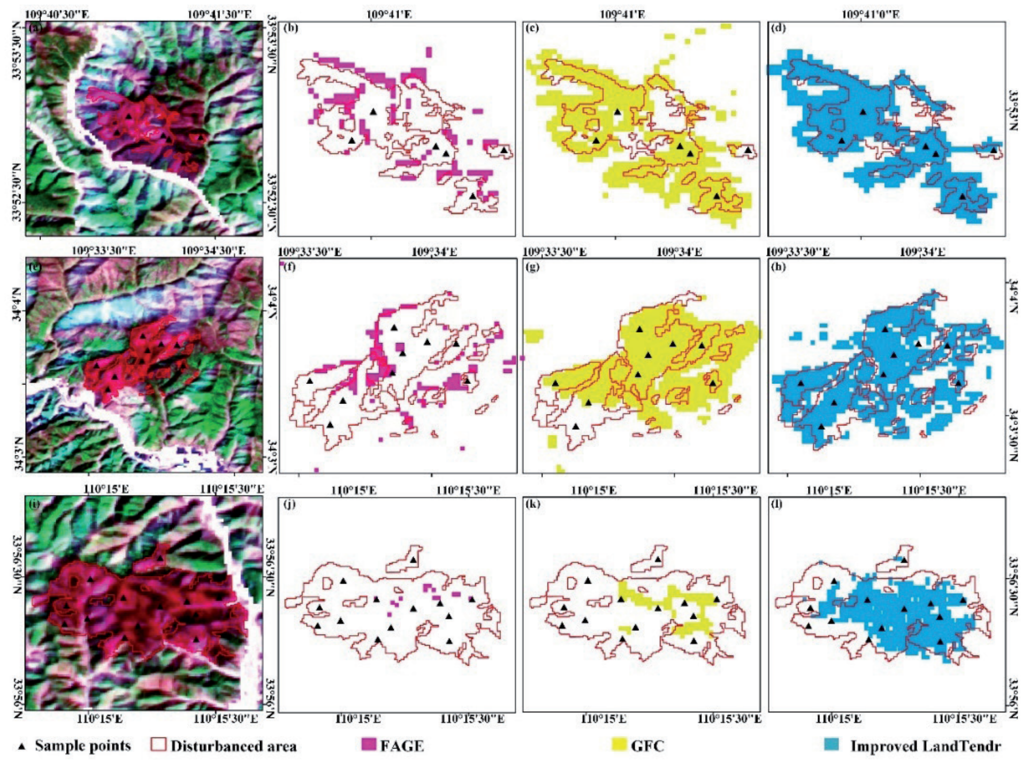

Fig. 7. Results of cross-validation among different product datasets.

disturbances, demonstrating the benefit of multi-source satellite fusion for enhanced spatial resolution in complex mountainous terrain.

In general, the accuracy evaluation shows that the enhanced LandTrendr workflow reliably detects forest disturbances in the Qinling Mountains in both temporal and spatial dimensions. Despite the structural limitations of annual time series reducing sensitivity to short-term or fast-recovering disturbances, the algorithm performs very well for moderate to severe disturbances, offering higher accuracy and consistency than standard global disturbance products.

Spatiotemporal Patterns of Forest Disturbances

Fig. 8 illustrates the overall spatial distribution of forest disturbances in the Qinling Mountains during 2014-2023. Statistical analysis indicates that during the last ten years, the study area experienced forest disturbances of varying intensities at different times, totaling 2.15×10^4 km^2. The most severe disturbance occurred in 2015, covering 2.53×10^3 km^2, or 11.78% of the total disturbed area. In the study area, the eastern, southern, and northwestern mountainous regions experienced more significant disturbances, whereas disturbances in the northern regions were more dispersed. Slopes within the study area were divided into six levels, and the annual forest disturbances in the Qinling Mountains were analyzed for each slope category. Between 2014 and 2023, most forest disturbances in the Qinling Mountains occurred on slopes less than 35°.

Forest disturbances within this slope range covered 2,173.916 km^2, representing 72.73% of the total disturbed area. Slopes between 15° and 25° had the highest disturbance area, amounting to 1,143.675 km^2. Disturbances occurring on slopes above 35° were minor, totaling 171.983 km^2, accounting for 5.75% of all disturbed areas. As slope increases, the disturbed area shows a decreasing trend. Elevation-based statistics indicate that forest disturbances predominantly occurred at mid- to low-elevations below 1,450 m.

Fig. 9c) presents the 2014-2023 trend of forest NBR index variation. Forest degradation primarily occurred in the northern and northeastern foothill areas of the Qinling Mountains, with central and southern regions having relatively sparse forest cover. In the last decade, forests exhibiting a "greening" trend were mainly located in the central and northwestern mountainous regions, with a total area of 6.13×10^4 km^2, representing 10.05% of the 2023 forest area. To gain a clearer understanding of the spatial patterns of forest disturbances in the Qinling Mountains over the last ten years, the study area was divided into 332 spatial grid units of 3 km × 3 km. Subsequently, disturbance patterns over the past decade were evaluated at the grid-cell scale. Fig. 9d) illustrates that disturbance intensity was higher in the eastern and southern parts of the Qinling Mountains, whereas the western and some southern regions showed lower disturbance intensity.

Discussion

In monitoring forest disturbances, methods based on single spectral features combined with fixed-threshold change detection are highly sensitive to the choice of spectral index [11]. This is primarily due to the fact that different spectral features have different sensitivities to particular types of forest disturbances. Previous research generally emphasizes spectral indices that are sensitive to canopy structure or green leaf area, which are categorized into three types: (1) raw spectral bands, e.g., near-infrared (NIR) and shortwave infrared (SWIR); (2) vegetation indices, e.g., NDVI, EVI, and NBR; and (3) tasseled cap transformation indices, e.g., tasseled cap greenness (TCG). Indices of different

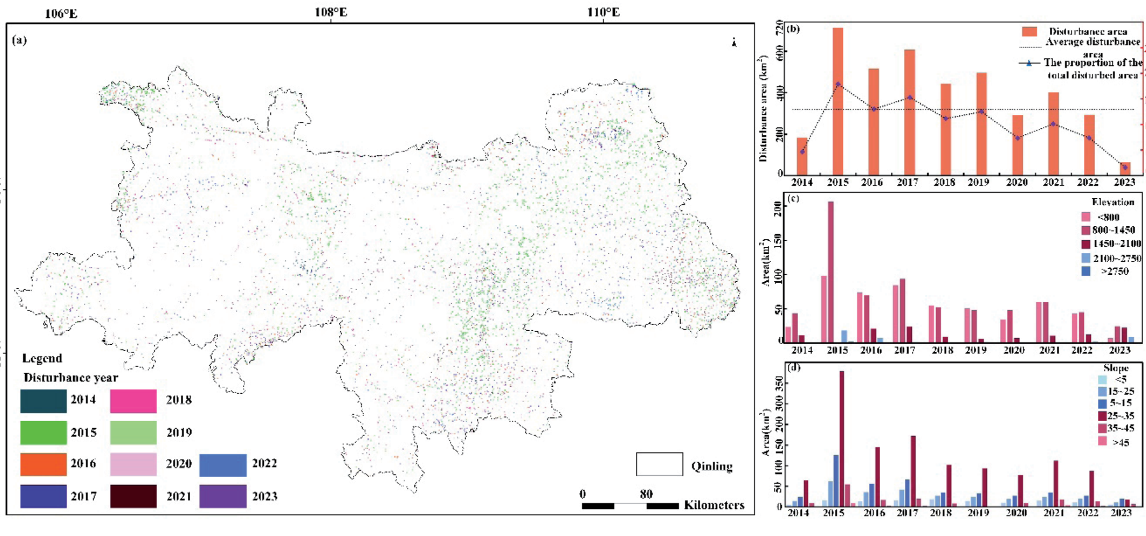

Fig. 8. Spatiotemporal distribution of extracted forest disturbance results.

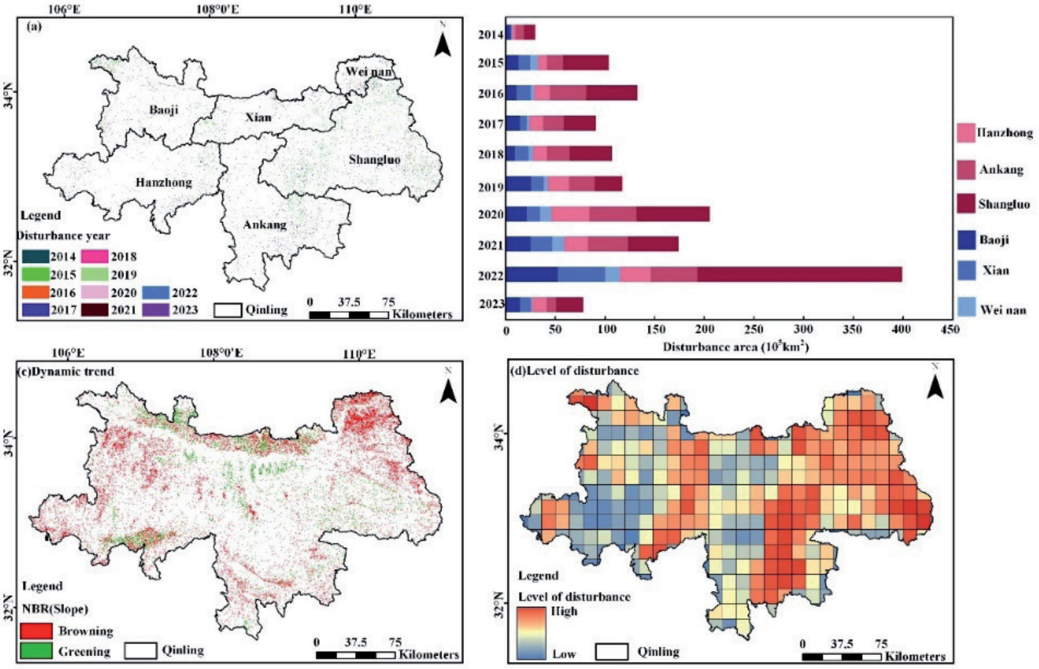

Fig. 9. Classification of forest disturbance intensity.

types exhibit distinct sensitivities to disturbance type, response timing, and disturbance intensity, making the choice of appropriate spectral indices essential for accurately detecting forest disturbances.

To evaluate how different spectral indices affect disturbance detection accuracy, a fire site from March 2019 was used as a case study, with annual time series of various spectral indices applied as input to the enhanced LandTrendr algorithm to analyze and compare disturbance extraction results. Initially, the annual time series trajectories of each spectral index were computed and fitted using piecewise regression. The results (Fig. 10) show that of the six spectral indices (NBR, NDVI, EVI, TCG, NIR, SWIR), vegetation indices performed better than tasseled cap and single-band approaches, effectively capturing abrupt disturbance events in the temporal sequence.

This is primarily because vegetation indices, by combining multiple bands, increase the contrast between vegetation greenness and background spectra, thereby

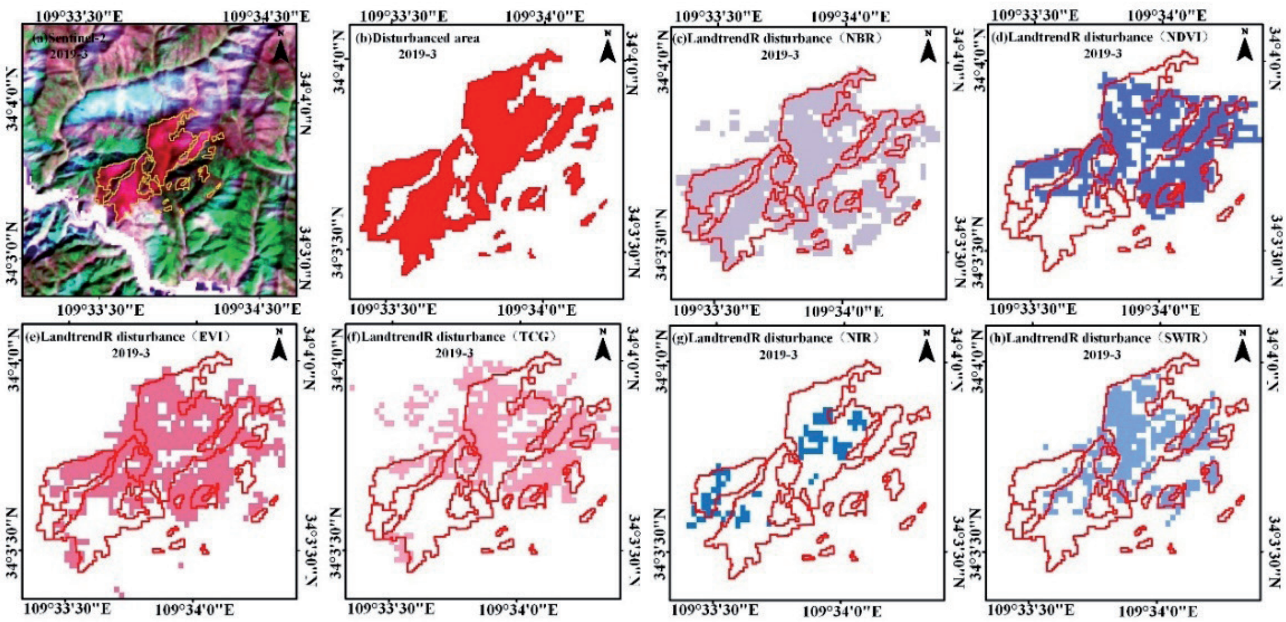

Fig. 10. Performance of different disturbance detection algorithms on disturbance extraction.

improving sensitivity to vegetation changes. In contrast, single-band indices are highly susceptible to terrain, atmospheric, and other external influences.

NBR exhibited the highest detection accuracy, whereas the NIR band performed the worst. NBR outperforms others because it is highly sensitive to vegetation chlorophyll, carbonized matter, and soil moisture. NDVI, EVI, and TCG more effectively capture vegetation physical characteristics, facilitating differentiation of disturbance types and intensities. The SWIR band is minimally influenced by atmospheric noise, effectively differentiates forest, soil, bark, and branches, and shows good performance in detecting fire and harvesting disturbances. The NIR band primarily represents canopy cellular structure, responds weakly to changes in leaf porosity and reflectance, and may easily lead to omissions under bare soil or variable moisture conditions.

Given the limitations of relying on a single vegetation index, to enhance the precision and robustness of disturbance identification, future research should combine multiple vegetation indices within the framework of multi-source satellite data fusion and optimized LandTrendr parameters, enabling more accurate monitoring and more efficient, reliable detection across various disturbance types and spatial scales.

Conclusions

This study presents a spatiotemporal monitoring approach for mountain forest disturbances using time-series spectral features obtained from multi-source satellite data fusion. This approach effectively overcomes the challenges of poor disturbance monitoring in mountainous areas due to persistent clouds and rain, enabling the generation of forest disturbance products with high spatiotemporal resolution.

(1) Integrating multi-source satellite data effectively resolves problems of persistent cloud cover and data gaps in complex mountainous terrain. The optimized control parameters considerably improve the LandTrendr algorithm's sensitivity for monitoring disturbances in mountainous areas. The produced disturbance products reached an overall accuracy of 96.51% and a Kappa of 0.908, exceeding the performance of current forest disturbance products.

(2) Between 2014 and 2023, the overall forest disturbance in the Qinling Mountains was moderate, covering about 4.01×10^3 km^2, which represents 7.1% of the 2023 forest area. Disturbances were primarily concentrated in the southern Qinling region, especially in Shangluo, predominantly occurring at elevations near 800 m and slopes around 25°. High-altitude forests were scarcely disturbed, reflecting relatively stable ecological conditions.

(3) Within the LandTrendr algorithm, the sensitivity of disturbance detection varies across spectral indices. NBR is particularly responsive to vegetation leaf chlorophyll and soil moisture, showing the greatest sensitivity and robustness, making it the most suitable index for detecting forest disturbances in mountainous settings.

However, several limitations should be noted. The classification relies on Landsat and Sentinel-1 imagery, which may still be affected by residual cloud contamination or radar noise. The 30 m spatial resolution may not capture fine-scale forest structural changes or small disturbances. In addition, training samples primarily derived from high-resolution imagery and existing products may introduce biases in underrepresented land cover types. Future studies could integrate additional high-resolution datasets and advanced machine learning methods to further improve forest disturbance detection.

Acknowledgments

This research was funded by the Shaanxi Academy of Forestry (Grant No. SXLK2022-02-13).

AI Usage Disclosure Statement

We confirm that AI tools (ChatGPT) were used solely for language polishing and grammatical improvement. No AI tools were used for data analysis, interpretation, or scientific writing. All scientific content and conclusions were made by the authors.

Conflict of Interest

The author declares no conflict of interest.

References

1. TERESA D.M., PFLUGMACHER D., BAUMANN M., LAMBIN E.F., GASPARRI I., KUEMMERLE T. Characterizing forest disturbances across the Argentine Dry Chaco based on Landsat time series. International Journal of Applied Earth Observation Geoinformation, **98**, 102310, **2021**.
2. HUANG C., GOWARD S.N., MASEK J.G., THOMAS N., ZHU Z., VOGELMANN J.E. An automated approach for reconstructing recent forest disturbance history using dense Landsat time series stacks. Remote Sensing of Environment, **114** (1), 183, **2010**.
3. ZHU Z., ZHANG J., YANG Z., ALJADDANI A.H., COHEN W.B., QIU S., ZHOU C. Continuous monitoring of land disturbance based on Landsat time series. Remote Sensing of Environment, **238**, 111116, **2020**.
4. FENG Y., ZIEGLER A.D., ELSEN P.R., LIU Y., HE X., SPRACKLEN D.V., HOLDEN J., JIANG X., ZHENG C., ZENG Z. Upward expansion and acceleration of forest clearance in the mountains of Southeast Asia. Nature Sustainability, **4** (10), 892, **2021**.

5. THOM D., SEIDL R. Natural disturbance impacts on ecosystem services and biodiversity in temperate and boreal forests. Biological Reviews, **91** (3), 760, **2016**.
6. YANG Y., ANDERSON M., GAO F., HAIN C., NOORMETS A., SUN G., WYNNE R., THOMAS V., SUN L. Investigating impacts of drought and disturbance on evapotranspiration over a forested landscape in North Carolina, USA using high spatiotemporal resolution remotely sensed data. Remote Sensing of Environment, **238**, 111018, **2020**.
7. COHEN W.B., YANG Z., STEHMAN S.V., SCHROEDER T.A., BELL D.M., MASEK J.G., HUANG C., MEIGS G.W. Forest disturbance across the conterminous United States from 1985–2012: The emerging dominance of forest decline. Forest Ecology Management, **360**, 242, **2016**.
8. GHADERPOUR E., PAGIATAKIS S.D., HASSAN Q.K. A survey on change detection and time series analysis with applications. Applied Sciences, **11** (13), 6141, **2021**.
9. HANSEN M.C., POTAPOV P.V., MOORE R., HANCHER M., TURUBANOVA S.A., TYUKAVINA A., THAU D., STEHMAN S.V., GOETZ S.J., LOVELAND T.R., KOMMAREDDY A., EGOROV A., CHINI L., JUSTICE C.O., TOWNSHEND J.R.G. High-resolution global maps of 21st-century forest cover change. Science, **342** (6160), 850, **2013**.
10. TOWNSHEND J.R., MASEK J.G., HUANG C., VERMOTE E.F., GAO F., CHANNAN S., SEXTON J.O., FENG M., NARASIMHAN R., KIM D., SONG K., SONG D., SONG X.-P., NOOJIPADY P., TAN B., HANSEN M.C., LI M., WOLFE R.E. Global characterization and monitoring of forest cover using Landsat data: opportunities and challenges. International Journal of Digital Earth, **5** (5), 373, **2012**.
11. HEMATI M., HASANLOU M., MAHDIANPARI M., MOHAMMADIMANESH F. A systematic review of landsat data for change detection applications: 50 years of monitoring the earth. Remote Sensing, **13** (15), 2869, **2021**.
12. VERBESSELT J., ZEILEIS A., HEROLD M. Near real-time disturbance detection using satellite image time series. Remote Sensing of Environment, **123**, 98, **2012**.
13. ZHU Z., WOODCOCK C.E. Continuous change detection and classification of land cover using all available Landsat data. Remote sensing of Environment, **144**, 152, **2014**.
14. PLATT R.V., OGRA M.V., BADOLA R., HUSSAIN S.A. Conservation-induced resettlement as a driver of land cover change in India: An object-based trend analysis. Applied Geography, **69**, 75, **2016**.
15. WANG Z., YAO W., TANG Q., LIU L., XIAO P., KONG X., ZHANG P., SHI F., WANG Y. Continuous change detection of forest/grassland and cropland in the Loess Plateau of China using all available Landsat data. Remote Sensing, **10** (11), 1775, **2018**.
16. COHEN W.B., HEALEY S.P., YANG Z., ZHU Z., GORELICK N. Diversity of algorithm and spectral band inputs improves Landsat monitoring of forest disturbance. Remote Sensing, **12** (10), 1673, **2020**.
17. DE JONG S.M., SHEN Y., DE VRIES J., BIJNAAR G., VAN MAANEN B., AUGUSTINUS P., VERWEIJ P. Mapping mangrove dynamics and colonization patterns at the Suriname coast using historic satellite data and the LandTrendr algorithm. International Journal of Applied Earth Observation and Geoinformation, **97**, 102293, **2021**.
18. RUNGE A., NITZE I., GROSSE G. Remote sensing annual dynamics of rapid permafrost thaw disturbances with LandTrendr. Remote Sensing of Environment, **268**, 112752, **2022**.
19. HAMUNYELA E., VERBESSELT J., HEROLD M. Using spatial context to improve early detection of deforestation from Landsat time series. Remote Sensing of Environment, **172**, 126, **2016**.
20. REICHE J., HAMUNYELA E., VERBESSELT J., HOEKMAN D., HEROLD M. Improving near-real time deforestation monitoring in tropical dry forests by combining dense Sentinel-1 time series with Landsat and ALOS-2 PALSAR-2. Remote Sensing of Environment, **204**, 147, **2018**.
21. XU X., LIN D., YANG Y., LIU J., ZOU C., LIN N., JIAO F., WU Q., QIU J., ZHANG K. Identification of degradation risk areas and delineation of key ecological function areas in Qinling region. Scientific Reports, **15** (1), 4374, **2025**.
22. DESROCHERS M.L., CLIPPARD E.A., JOHNSON L.K., BEIER C.M. Declining trends in canopy disturbance across reserve forest landscapes of the northeastern US. Forest EcologyManagement, **578**, 122463, **2025**.
23. AWTY-CARROLL K., BUNTING P., HARDY A., BELL G. An evaluation and comparison of four dense time series change detection methods using simulated data. Remote Sensing, **11** (23), 2779, **2019**.
24. COHEN W.B., HEALEY S.P., YANG Z., STEHMAN S.V., BREWER C.K., BROOKS E.B., GORELICK N., HUANG C., HUGHES M.J., KENNEDY R.E., LOVELAND T.R., MOISEN G.G., SCHROEDER T.A., VOGELMANN J.E., WOODCOCK C.E., YANG L., ZHU Z. How similar are forest disturbance maps derived from different Landsat time series algorithms? Forests, **8** (4), 98, **2017**.
25. VOGELMANN J.E., GALLANT A.L., SHI H., ZHU Z. Perspectives on monitoring gradual change across the continuity of Landsat sensors using time-series data. Remote Sensing of Environment, **185**, 258, **2016**.
26. GAO F., HILKER T., ZHU X., ANDERSON M., MASEK J., WANG P., YANG Y. Fusing Landsat and MODIS data for vegetation monitoring. IEEE Geoscience Remote Sensing Magazine, **3** (3), 47, **2015**.
27. WU L., LI Z., LIU X., ZHU L., TANG Y., ZHANG B., XU B., LIU M., MENG Y., LIU B. Multi-type forest change detection using BFAST and monthly landsat time series for monitoring spatiotemporal dynamics of forests in subtropical wetland. Remote Sensing, **12** (2), 341, **2020**.
28. HERMOSILLA T., WULDER M.A., WHITE J.C., COOPS N.C., HOBART G.W. Regional detection, characterization, and attribution of annual forest change from 1984 to 2012 using Landsat-derived time-series metrics. Remote Sensing of Environment, **170**, 121, **2015**.
29. LIU Z., ZHANG Y., ZHENG X. Improving Urban Forest Expansion Detection with LandTrendr and Machine Learning. Forests, **15** (8), 1452, **2024**.
30. COHEN W.B., YANG Z., KENNEDY R. Detecting trends in forest disturbance and recovery using yearly Landsat time series: 2. TimeSync—Tools for calibration and validation. Remote Sensing of Environment, **114** (12), 2911, **2010**.